JOURNAL OF MATERIALS SCIENCE 37 (2002) 4865–4870

An experimental investigation of failure behavior of conducting polythiophene coating films

XI-SHU WANG*, YAN-HONG DENG, YONG-QIANG LI
Department of Engineering Mechanics, Tsinghua University, Beijing 100084, People's Republic of China
E-mail: xshwang@mail.tsinghua.edu.cn

Polymeric films with different conductivities are widely used as coatings on electronic devices. For the reliability of their application, evaluation of mechanical properties is essential. In this paper, mechanical properties of conducting polythiophene (Pth) films are investigated with Scanning Electron Microscopy (SEM) to understand the relation between the mechanical properties and the electrochemical polymerization (ECP) deposition process and microstructure as well as film thickness. An attempt to explain the special properties exhibited by films with different thickness is made. The fatigue microcrack initiation and growth around a cross indent was observed in low cycle tension-tension fatigue tests. Three typical fatigue fracture models (short micro crack propagation, spallation and fragmentation) for films deforming coherently with the stainless steel substrate have been directly observed with SEM and conditions for their occurrences are discussed.

1. Introduction

Owing to the rapid development in techniques of manufacturing conducting polymers [1, 2], it has become possible to control the electrical property of polymers over the range from insulator to fine conductor. Some polymeric materials have successively been synthesized with conductivity similar to metals like copper [3]. Various types of synthesized polymers are joining the family of conductors previously dominated by metals. In addition, conducting polymers exhibit some properties that are superior to conventional conductors such as low density, ease of fabrication, flexibility in design, and resistance to corrosion. Therefore, they may be used in various applications as substitutes for metals [4].

The promise of combining these properties with good electrical properties in polymers has prompted extensive research interest in the last two decades. However, most of the previously synthesized conducting polymers are brittle, insoluble, intractable, and often decompose before melting [5]. The preparation of conducting polymers with high strength and good chemical stability remains a great challenge.

Nowadays, investigations on the relationship between the macroscopic properties and microstructures of conducting polymer films are scarcely done. Recently, polythiophene coating films with high conductivity and chemical stability have been synthesized by an electrochemical method [6, 7]. The mechanical properties of these films were experimentally investigated with electronic speckle pattern interferometry (ESPI) and SEM. Significant effects of thickness on the strength and Young's modulus and other mechanical properties of films are found [8, 9]. In this paper, we try to give an explanation by studying the microstructure (i.e. the deposition mechanism) for the effects. In addition, the fracture mechanism of polythiophene coating films deforming coherently with the substrate is also discussed using experimental method with SEM.

2. Electrochemical sythesising of polythiophene films

The polythiophene (Pth) thin film was synthesized in a one-compartment cell with the use of an EG&G potentiostatic model 283 under computer control that is called the three-electrode system consisting of working-, counter- and reference-electrode. The working-electrode acts as the substrate for electrodeposition of Pth. Since the deposition of the polymeric films is an oxidative process, it is necessary that the electrode does not oxidize concurrently with the aromatic monomer. For this reason only, inert electrodes like stainless steel substrates were used. The working- and counter-electrodes were AISI 304 stainless steel sheets ($L \times W \times t$: 45 mm × 2.5 mm × 1 mm) placed 5 mm apart. The reference electrode was Ag/AgCl. The electrolyte solution was freshly distilled boron fluoride-ethyl etherate $[BF_4]^-$ containing 30 mM thiophene at a constant potential of 1.3 V [7]. All residual solutions were deaerated by a dry argon stream and maintained at a light overpressure during fabricating. The total charges exchanged during the deposition process were

*Author to whom all correspondence should be addressed.

used to control the thickness of the deposited films. All films were washed with distilled ethyl ether and dried under vacuum at 80°C for about 24 hours.

3. Fatigue experimental procedure

Fig. 1 shows the geometry of the sample used in fatigue tests. In the middle of each sample, a through-film indention was impressed. Observations of fatigue microcrack initiation and propagation were then focused on the two tips of the indention.

The applied stress in the experimental process means a nominal one that is calculated neglecting the presence of the Pth coating film layer. Assuming the deformation of the Pth coating film is equal to that of the surface substrate, the strain of the film can be denoted as

$$\varepsilon_f = \varepsilon_s = \frac{\sigma_s}{E_s} \tag{1}$$

and the loading to which the coating film is subjected as

$$\sigma_f = E_f \varepsilon_f = \frac{E_f}{E_s}\sigma_s \tag{2}$$

where $\varepsilon_f, \sigma_f, E_f$ represent the strain, stress and Young's modulus of the coating film and $\varepsilon_s, \sigma_s, E_s$ represent the strain, stress and Young's modulus of the substrate. We note that this relation, which correlates the stress applied upon the Pth coating film and that upon the substrate, cannot include the interaction of the coating film and substrate. So, it is necessary to determine the limiting stress at which the film detaches from the substrate in order to avoid the film detaching from the substrate before the fatigue testing. A simple three-point-bending test in the fatigue test machine with the SEM (Shimadzu corporation Kyoto Japan) just meets the demand. The formula that we employed was given by Nix [10], with which the stress in the film (regarded as uniformly distributed along the thickness of the film), as well as the limiting stress we expected, can be determined by the curvature of the substrate (or the film) subjected to bending loading. The equation is given below:

$$\sigma_f = M_s \frac{h_s^2}{6h_f R} \tag{3}$$

where $M_s = E/(1-\upsilon)$ is the biaxial elastic modulus of the substrate, h_f, the thickness of the film, and h_s, the thickness of the substrate. When $\sigma < \sigma_f$, the deformation of the coating film approximately equal to that of the substrate under cyclic loading. Through this test, the stress amplitude for fatigue tests can be estimated.

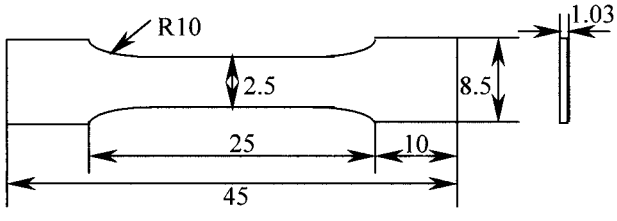

Figure 1 The shape and size of polythiophene coating film on the substrate.

It should be noted that Equation 3 for the elastic bending of the substrate does not depend on the elastic properties or any other mechanical properties of the film. The reason for this relates to the thin film approximation that is made in the derivation of this result. Typically, films about 1-μm thick are deposited onto substrates that may be 50 to 100 times thicker and more than. In such cases, the flexural modulus of thin film/substrate composite is completely dominated by the properties of the substrate and the properties of the thin film have a negligible effect on the bending. It follows that when multiple thin films are deposited sequentially onto a much thicker substrate, each film causes a fixed amount of bending to occur, irrespective of the order in which the films are deposited. The amount of curvature change is determined by the stress and thickness of each film. The total change of substrate curvature is simply the sum of the curvature changes associated with the presence of each film. Of course, the sign of the curvature change caused by each film must be taken into account. For cases in which the films are not thin compared to the substrate, a more elaborate bending analysis must be used that takes account of the elastic properties of the films [11].

Under fatigue loading, microcracks grew from the tip of the indent and the microcrack length was measured with the SEM and defined as the crack length including the indent size. The fatigue microcrack initiation and propagation tests were performed in the vacuum chamber of the SEM using a specially designed servo-hydraulic testing system under cyclic loading operating at 10 Hz of ± 1 kN capacity. The electron signal of the SEM was directed to the main memory of the microcomputer through direct memory access A/D converter with digitizing rate of 33 msec per picture. Successive 960×1200 frames of the SEM image data under cyclic tension-tension loading of less than 0.5 Hz can be obtained easily. These tests were carried out at about $R = 0.1$ and all microcracks initiated and propagated are observed at about 0.1 Hz.

4. Results and discussions

4.1. Fracture analysis for conducting Pth films in different thickness

Recently, Pth and polypyrrole (PPy) thin films with medium conductivity and chemical stability have been synthesized by an electrochemical method [6, 7]. Wang and co-workers investigated experimentally the mechanical properties of conducting Pth coating films with the ESPI and the SEM methods [8, 9]. According to their results, the Young's modulus decreases rapidly as the thickness increases within 10 μm, but approaches to a constant value when the thickness exceeds such a threshold. In other words, the dependence of the Young's modulus upon the thickness includes two regimes, a constant regime for thickness larger than about 10 μm, and a decreasing regime with smaller thickness.

The SEM images in Fig. 2 are two fracture surfaces of conducting Pth films after static tensile fracture tests. In Fig. 2a, the cross section of the film includes two distinct regions in microstructure in the 65 μm-thick

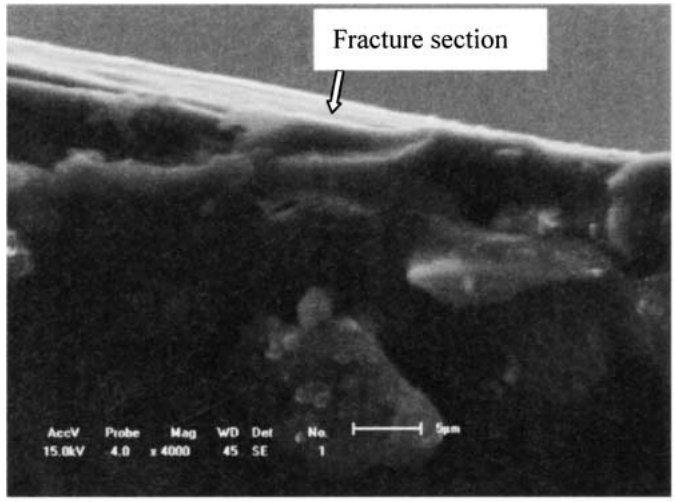

(a)

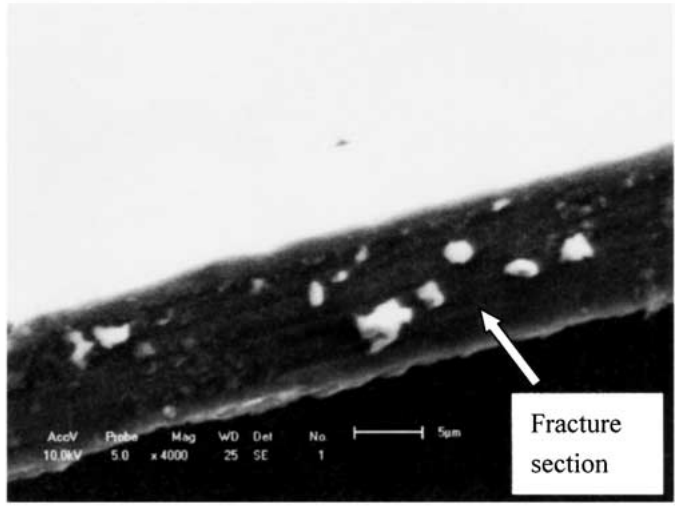

(b)

Figure 2 SEM images of fracture surface of polythiophene films. (a) Fracture surface of 65 μm thickness film. (b) Fracutre surface of 10 μm thickness film.

film. One region close to the substrate formed a dense layer (the white layer), in which there were few flaws as seen in Fig. 2a. Another region close to the free surface deposited a porous layer (the fuscous layer). At the same time, it is clearly seen that there are a few voids and more agglomerated grains in the fuscous layer. These microstructures lead to their strengths per unit thickness to become weaker. Fig. 2b shows the fracture surface of a 10 μm-thick Pth film which was observed in the same testing conditions as that of the 65 μm-thick film. As is mentioned above, there are few flaws on the fracture surface of 10 μm-thickness film. When the film is thicker than about 5–7 μm, the microstructure is different as seen in Fig. 2a. The reason for such a difference in microstructure was attributed to the growth of the film in thickness by Wang and co-workers [8]. However they did not give a detailed explanation of the growth mechanism.

Actually, it is easy to explain in terms of the deposition mechanism of thin films. At the beginning of the potentiostatic deposition process, the thiophene molecules assemble into "islands" along the surface of the working electrode (stainless steel plate or other electrode plate). These islands are compact because of the higher voltage between the plane where they deposit and the reference electrodes (in the three-electrode system). But as the islands grow larger (i.e. the film grows thicker), the voltage decreases and consequently larger and looser agglomerates are formed. In the final stage of deposition, the spaces between the islands are then covered by layers that extend throughout the plane. This is clearly shown in Fig. 3. Such a deposition process is very similar to the Volmer-Weber model or the VWBD theory [12–16] that was proposed for deposition of metal films. As a consequence of the electrochemical synthesis process, the microstructure of a conducting Pth coating film varies significantly with the increase of the thickness. Microcracks caused by the heterogeneity and the residual stress can be seen to be found in the 65 μm-thick polythiophene film by the SEM (Fig. 4).

Another source for microcracks is the residual stresses caused by thermal mismatch during the desiccation process. Given the change of temperature, the thermal stress can be formulated as

$$\sigma_t = E_f \Delta\alpha \Delta T \tag{4}$$

where E_f is the elastic modulus of the film, $\Delta\alpha = \alpha_f - \alpha_s$, α_f, α_s are linear thermal expansion factors of film and substrate respectively, ΔT is the change

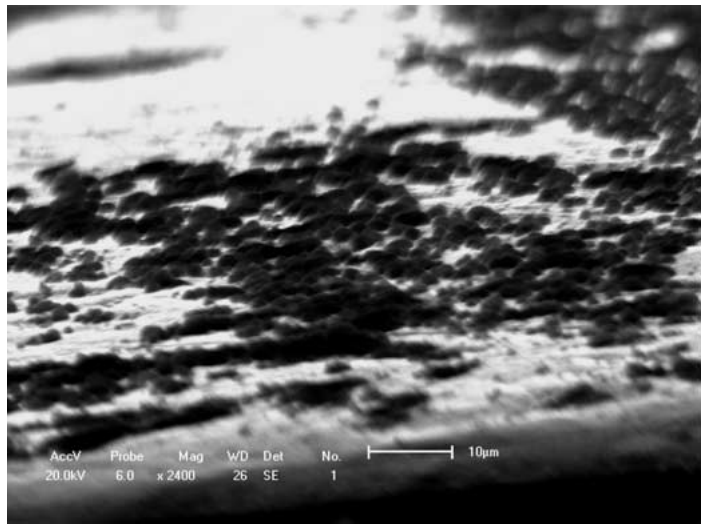

Figure 3 SEM image of island structure section of 10 μm thickness film.

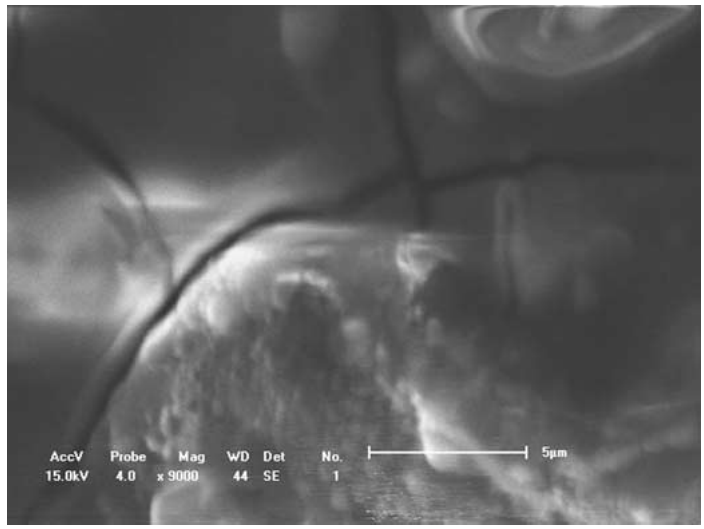

Figure 4 SEM image of microcracks caused the residual stress in a conducting Pth film.

of environmental temperature. A typical case is one in which a Pth film is deposited onto stainless steel substrate in a stress-free state at higher temperatures and subsequently cooled at room temperature. In such cases, $\Delta\alpha > 0$ and $\Delta T < 0$ so that the elastic accommodation strain is positive and tensile stresses are developed in the film and subsequently form microcracks on the free surface of the Pth coating film as shown in Fig. 4 (The film is 65 μm in thickness). Following Wang's results for elastic modulus of films, it seems that the thinner the film is, the less is the residual stress which may occur for same change of temperature [9]. However, it does not necessarily follow, because different thickness can also lead to different linear expansion coefficients. A definite answer to this "discrepancy" is that when the thickness of a film is more than about 30 μm, microcracks inevitably occur because of the thermal energy enclosed deep inside the film. In addition, for thinner film, it is easy for the molecule islands to move along the substrate or for smaller agglomerative molecule islands to form on the substrate easily. So the internal/residual stress is not easily produced. But as the film thickness increases, the probability of producing internal/residual stress increases as well. The reliability of film-coated devices may be determined by these micro defects introduced in the process of deposition. Therefore, improvement in the existing electrochemistry synthesis process is necessary in order to obtain the Pth films with better mechanical properties and conductivities. Quantitative investigations on the mechanical or electric properties-microstructure relationship of conducting coating films are really indispensable for the practical application of thin films in industry. The studied reports from the viewpoint of the relationship between microstructure or the electrochemical syntheses of conducting polymer coating film and electric and mechanical properties will be seen shortly afterwards. Detailed discussion of the effect of residual stress on the microcracks and residual stress development of polymer coating film can be seen in references [17, 18].

4.2. Fatigue fracture properties of conducting Pth coating film

Direct observation of fatigue fracture properties was carried out with samples as shown in Fig. 5 at different stress under constant amplitude cyclic loading. The depth of indentation is about 20 μm. When the stress

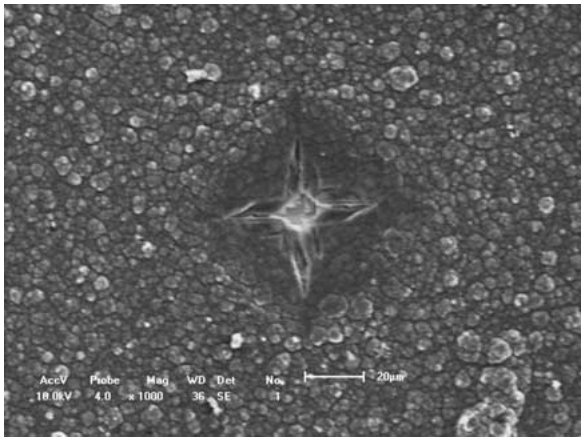

Figure 5 Indenter impression on the surface of coating film.

amplitude is so high that the Pth film withstands a deformation from the substrate, the two tips of the indention in the width direction will have a stress intensity factor ΔK_I. The microcrack initiation or propagation may occur ahead of the tips. Owing to the visco-elastic property of the coating and an effect of the adhesive force, the fatigue microcrack propagates little in spite of the occurrence of greater microcrack opening displacement, and it is difficult to express the microcrack growth rate with ΔK_I. The propagation of microcracks will be our focus in further research. Besides, other fatigue damage types of the conducting polythiophene coating film on the substrate may occur such as decohesion, spallation and fragmentation etc. [19].

Fig. 6a shows that one of the fatigue fracture types at the edge of the sample occurs after about 4×10^4 cycles under the applied stress range $\Delta\sigma_f = 1.73$ MPa in $R = 0.1$. As the coating film is subjected to cyclic deformation, the adhesive force between the coating film and the substrate decreases as the fatigue test progresses, and the distributed adhesion stress is not uniform in the surface of sample. An example of the spallation type is shown in Fig. 6a. Accompanying spallation, a few fragments as well as some shorter microcracks occur because, near the crack tip, the film does not receive enough stress from the substrate for propagation of longer cracks. The adhesion of the coating film on the stainless steel substrate is weaker than on other substrate materials. Therefore, in this experimental observation process, the spallation is the main fatigue failure type in this experimental condition. Now, we can determine the amounts of the adhesive force used in above mention an experimental method [10], analyze/explain the fatigue fracture process with the equilibrium theory of misfit dislocation formation [20–23], and evaluate the effect of the adhesion force on the fatigue failure of the coating film on the substrate.

Fig. 6b shows that fatigue fragmentation occurs when samples are under stress amplitude of $\Delta\sigma_f = 1.73$ MPa in $R = 0.1$ and after about 8×10^4 cycles. When the adhesive force per unit area on a surface coating film is less than that in the stress concentration on the surface coating film, a fatigue fragment will occur. So the fatigue failure for the conducting Pth coating film on the stainless steel substrate displays a mixed fatigue failure

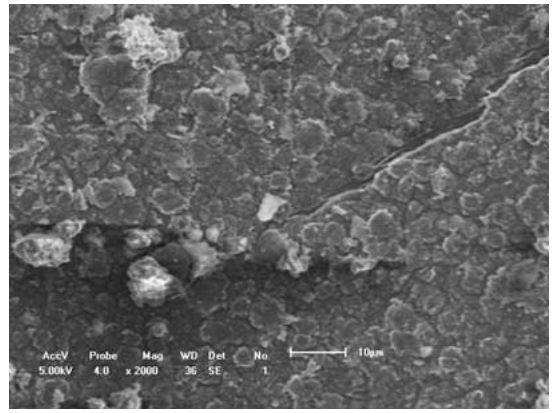

(a)

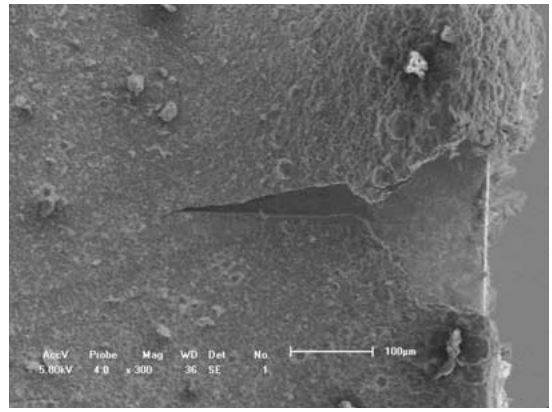

(b)

Figure 6 Fatigue fracture types of a conducting Pth coating film on a substrate. (a) A spalling fracture type caused by fatigue loading. (b) A fragmentation fracture type caused by fatigue loading.

type. Therefore, how to evaluate these fatigue fracture types will be one of our main works in the future.

5. Concluding remarks

The performed investigations proved the fracture behavior as well as stresses in the coating films on the stainless steel substrates with experimental methods. This study leads to an understanding of the electrochemical deposition mechanism of polymer coating film on the substrates and the effect of the microstructure of polymer coating film on its mechanical properties. According to our experimental and analytical results, the tensile strength of the conducting Pth films is optimal when the uniform film is thinner than 10 μm, because the heterogeneous microstructure causes profuse microdefects and residual stresses in thicker films. To obtain the higher strength of conducting Pth films thicker than 10 μm with better quality, the polymerization process needs to be improved to yield a stable and uniform growth of films.

We have also shown that the results of fatigue failure behavior of the conducting Pth coating film on the stainless steel plate were observed with the SEM techniques. The fatigue testing results clearly show that the conducting Pth film on the substrate occurs the fatigue failures when the cyclic umbers reached at 4×10^4–8×10^4 cycles though the applied stress under the fatigue testing is less than the limit stress. The fatigue

fracture types of conducting Pth coating film were obtained from the SEM images of samples under cyclic loading.

In order to explain in more detail the effect of the electrochemical synthesis process and the polymer microstructure on the mechanical properties/behaviors, we are now investigating at one hand. These results will be reported later.

Acknowledgements

The authors thank Prof. Gaoquan Shi's group in the Department of Chemistry at Tsinghua University for their help. The project is supported by the Basic-Research Foundation of Tsinghua University (JC2000057).

References

1. K. GURUNATHAN, A. V. MURUGAN, R. MARIMUTHU, U. P. MULIK and D. P. AMALNERKAR, *J. Mat. Chem. Phys.* **61** (1999) 173.
2. W. D. GILL, T. C. CLARKE and G. B. STREET, *J. Appl. Phys. Commun.* **2** (1982) 211.
3. S. N. BHADANI, S. K. SEN CUPTA and J. PRASAD, *J. Appl. Polym. Sci.* **47** (1993) 1215.
4. G. WEGNER, *Angew Chem. Int. Ed. Engl.* **20** (1981) 361.
5. S. LI, C. W. MACOSCO and H. S. WHITE, *J. Science* **259** (1993) 957.
6. G. SHI, C. LI and Y. LIANG, *J. Adv. Mater.* **11** (1999) 1145.
7. G. SHI, S. JIN, G. XUE and C. LI, *J. Science* **267** (1995) 994.
8. XISHU WANG and XIQIAO FENG, *J. Mater. Sci. Letts.* **21** (2002) 715.
9. XISHU WANG, JIAXIN ZHANG, SUIQUN ZHU and GAOQUAN SHI, *Acta Mechanica Solida Sinica* **15**(1) (2002) 30.
10. W. D. NIX, *Metallurgical Transactions* A **20A** (1988) 1989.
11. P. H. TOWNSEND, D. M. BARNETT and T. A. BRUNNER, *J. Appl. Phys.* **62** (1987) 4438.
12. M. VOLMER and A. WEBER, *Z. Phys. Chem.* **119** (1925) 277.
13. R. BECKER and W. DORING, *Ann. Phys.* **24** (1935) 719.
14. M. VOLMER, *Z. Electrochem.* **35** (1929) 555.
15. G. M. POUND, M. T. SIMNAD and L. YANG, *J. Chem. Phys.* **22** (1954) 1215.
16. K. KONTTURI, M. POHJAKALLIO, G. SUNDHOLM, E. VIEIL, *J. Electroanaly. Chem.* **384** (1995) 67.
17. GU YAN and J. R. WHITE, *Polym. Eng. Sci.* **39** (1999) 1856.
18. GU YAN and J. R. WHITE, *Polym. Eng. Sci.* **39** (1999) 1866.
19. XISHU WANG, SUIQUN ZHU, JIAXIN ZHANG and GAOQUAN SHI, in 8th Intersociety Conference on Thermal and Thermomechanical Phenomena in Electronic System-Itherm 2002, San Diego, USA.
20. J. H. VAN DER MERWE, *J. Appl. Phys.* **34** (1963) 123.
21. J. W. MATTHEWS and A. E. BLAKESLEE, *J. Cryst. Growth.* **29** (1975) 273.
22. J. W. MATTHEWS, *J. Vac. Sci. Technol.* **12** (1975) 126.
23. J. W. MATTHEWS and A. E. BLAKESLEE, *J. Cryst. Growth.* **27** (1974) 118.

Received 16 April
and accepted 16 April 2002